

Island Size and Environment Dependence of Adatom Capture: Cu/Co Islands on Ru(0001)

M. C. Bartelt,¹ A. K. Schmid,¹ J. W. Evans,² and R. Q. Hwang¹

¹Sandia National Laboratories, Livermore, California 94550

²Department of Mathematics and Ames Laboratory, Iowa State University, Ames, Iowa 50011

(Received 10 November 1997)

We quantify the rate of capture by Co islands on Ru(0001) of additionally deposited Cu atoms, using scanning tunneling microscopy. The dependence of the capture rates on Co-island size is shown to reflect larger island-free areas surrounding bigger islands, a feature neglected in mean-field treatments. We also find a strong direction dependence in Cu adatom capture, reflecting the local environment of individual islands. These features are elucidated by simulations and diffusion equation analyses. [S0031-9007(98)06845-8]

PACS numbers: 68.35.Fx, 61.16.Ch, 68.55.-a, 82.20.Mj

A broad range of fundamental processes are mediated by diffusion, including coagulation, aggregation, or chemical reaction in the fluid phase, and nucleation and growth during deposition. General analysis of these processes originated with the rate equation approach of Smoluchowski for the evolution of populations of clusters of various sizes [1,2]. A key component in this formalism is the specification, often invoking simple approximations, of rate “kernels” which depend on cluster size. An important application considered here, where the possibility arises for experimental determination of these kernels, is provided by metal-on-metal film growth under controlled ultrahigh vacuum (UHV) conditions.

Such metal film growth often proceeds via nucleation, growth, and subsequent coalescence of two-dimensional islands in each layer [3]. A precise description of island formation and growth is thus essential to reliably predict and characterize the resulting film morphology and related properties. Island growth is regulated primarily by the rate at which islands capture diffusing adatoms. The average capture rate for islands of size s (which have a variety of local environments) defines the “capture number” σ_s for aggregation. Specifically, the rate of decrease in the number density N_s of islands of size s , due to aggregation with diffusing adatoms, of density N_1 and hop rate h , equals $h\sigma_s N_1 N_s$. The behavior of σ_s is typically analyzed at a mean-field (MF) level, where the environment of each island is assumed independent of island size and shape [4]. Despite this fact, it has long been recognized that the island growth rate, and thus capture rate, reflect the area of the island-free region surrounding the islands. However, recent simulations of an idealized point-island model suggested that the variation of σ_s with s differs qualitatively from MF predictions [5]. Furthermore, it was shown that this size dependence controls the form of the island size distribution [5]. However, there have been no experiments tailored to address these issues, or analyses of realistic simulation models to provide some context in which to interpret experimental behavior.

In this Letter, we present the first experimental characterization of the island size dependence of adatom capture

and island growth. Specifically, we examine diffusion-mediated capture of deposited Cu adatoms by Co islands on Ru(0001). We find a strong size dependence, bigger islands having larger capture rates. This dependence reflects the existence of larger empty regions surrounding bigger islands, i.e., a strong correlation between island sizes and separations, ignored in MF analyses. In addition, limited rearrangement of Cu around the Co islands allows assessment of the direction dependence of capture and growth. We quantify these features for the experimental island distribution using both (i) stochastic simulations of capture of randomly deposited and diffusing atoms and (ii) deterministic diffusion equation analyses. Finally, we compare the observed behavior with the *qualitatively* similar predictions from simulations of irreversible formation of hexagonal islands. These predictions provide an essential benchmark for the interpretation of this and future experiments.

The experiments were performed in a UHV chamber (base pressure $<10^{-10}$ Torr) equipped with a scanning tunneling microscope (STM). Imaging was done at RT, in constant current mode, typically less than 1 hour after deposition. Coverages (θ), in monolayers (ML), were determined from the substrate area covered in the STM images (with uncertainty <0.05 ML). Knowledge of the evaporation time then yielded deposition rates.

We first deposited ~ 0.12 ML of Co on Ru(0001) at 50°C , by direct current heating of a Co wire, producing a distribution of pseudomorphic Co islands with irregular, threefold symmetric growth shapes and density $N_{\text{av}} \sim 130 \mu\text{m}^{-2}$ [6,7]. To facilitate comparison with simulation results for compact islands, we flash annealed the sample to 350°C . This equilibrated the island shapes without significantly coarsening the island distribution, as assessed by direct inspection and quantitative analysis of island sizes, positions, and island-pair densities and separations of large preannealed and postannealed images. However, some of the smallest islands are lost in the anneal.

To characterize the island size and environment dependence of adatom capture for this distribution of Co islands, we then deposited ~ 0.23 ML of Cu at RT from

a resistively heated tungsten basket. The choice of Cu has some clear advantages. At +0.6 V sample bias and 0.2–2 nA constant tunneling current, Co regions appear 0.7 Å lower than neighboring Cu regions, providing contrast between the two metals in Fig. 1(b). Also, the large diffusion length of Cu adatoms on Ru(0001) [6] prevents nucleation of new islands.

Roughly 85% (the fraction of uncovered substrate) of deposited Cu attached to the perimeter of the Co islands, forming a “ring”; see Fig. 1(b). The rest nucleated second-layer Cu islands, pointing to significant effective barriers for interlayer diffusion in this system at RT. These islands are found on top of Co (most near one type of island edge), consistent with the existence of an additional barrier for diffusion of second-layer Cu adatoms outward across the interface from Co to Cu. This interface remains unaltered and sharp. At RT, interface mixing in this system occurs on much longer time scales [8].

Remarkably, due to limited restructuring of the Cu rings around the Co islands, Fig. 1(b) gives information not only on the amount of Cu captured by each island but also on the direction from which most diffusing Cu adatoms approached the island. In particular, island edges facing wider island-free regions typically captured more Cu, while islands with more uniform denuded areas show more uniform Cu rings. This is clear evidence that the local environment of a Co island controls its growth rate.

The amount of Cu added to each Co-island perimeter is a measure of the corresponding σ_s , strictly speaking integrated over a finite increment of island size. (We show below that this integration does not significantly influence the s dependence of σ_s .) Some uncertainty in σ_s results from Cu atoms which deposited on top of the growing islands, diffused to the edge, and subsequently stepped down and attached to the island perimeter. However, this contribution cannot exceed ~ 0.01 ML, considering the “large” amount of second-layer Cu. We also assume that no significant coarsening of the adlayer (e.g., transfer of Co or Cu from small to big islands) took place before STM imaging (although loss of small islands is

possible). This would contribute to an apparent bias in adatom capture by the larger islands. We note in this regard that STM images taken hours later still show no apparent changes in island configuration.

Figure 2(a) shows the σ_s/σ_{av} versus s/s_{av} , where $s_{av} \approx \theta/N_{av}$ is the average island size, and σ_{av} is the average capture number for aggregation (averaged over all island sizes). One finds a “plateau” below $s \approx s_{av}$, followed by a quasilinear increase of σ_s with s for larger islands. This form reflects the feature that the first islands nucleated tend to have larger capture areas than newer islands, but as the latter grow they effectively transfer capture areas from smaller to larger sizes, creating the plateau. This behavior is analogous to that reported for a simple simulation model of epitaxy [5], but is qualitatively distinct from self-consistent MF predictions [9]. One can also obtain “direct capture numbers” Ω_s , for islands of size s , from the amount of Cu deposited on top of each island. We find expected linear dependence of Ω_s on s .

Simulations incorporating adatom deposition (at rate F), diffusion (at rate h) and subsequent irreversible capture by a distribution of islands matching experiment successfully fit the observed σ_s (and Ω_s); see Fig. 2(a). In the simulations, we used large $h/F = 10^{12}$, since diffusing adatoms are then more likely to aggregate with existing islands than to meet and nucleate new islands. We also utilized these simulations to show that averaging over a finite increment of island size, as in the experiment, does not change the form of σ_s/σ_{av} versus s/s_{av} .

To quantify the relation between adatom capture and the local environment of the islands, we first examined the dependence on island size of the area of cells in a Voronoi tessellation of the adlayer. Each Voronoi cell (VC) corresponds to the region of the surface closer to the center of mass (CM) of an island than to those of other islands [10]. Voronoi cells were chosen with the expectation that atoms deposited nearest to an island are more likely to aggregate with that island [5,11]. If A_s denotes the mean area of cells associated with islands of size s , then the average cell area, A_{av} , in units of

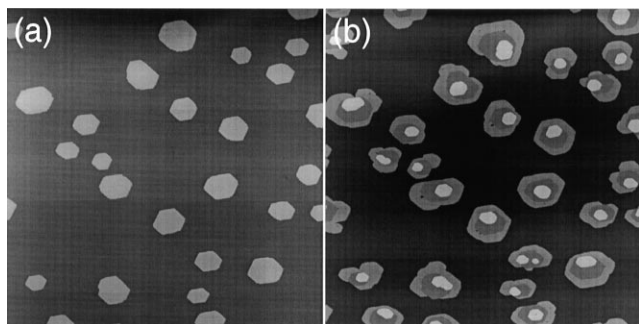


FIG. 1. $(500 \text{ nm})^2$ STM images of the same area. (a) ~ 0.12 ML of Co deposited on Ru(0001) at 50 °C and $\sim 2.4 \times 10^{-3}$ ML/s, followed by a flash anneal to 350 °C. (b) After deposition of ~ 0.23 ML of Cu (lighter areas); hours later, at RT and $\sim 3.9 \times 10^{-2}$ ML/s. Brighter regions represent higher surface regions.

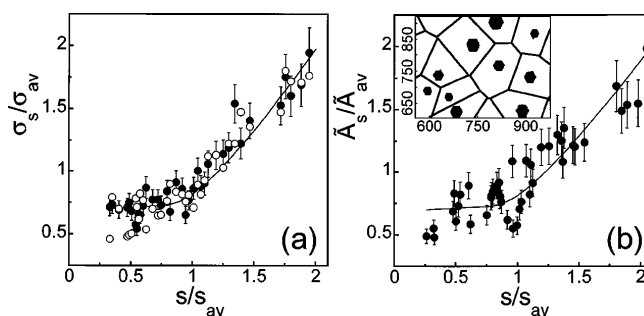


FIG. 2. Analysis of a $(1.2 \mu\text{m})^2$ STM image, partly shown in Fig. 1. Solid symbols are experimental data. Open symbols are simulation results ($h/F = 10^{12}$; 50 runs). Lines are simple fits. (a) σ_s/σ_{av} versus s/s_{av} . (b) A_s/A_{av} versus s/s_{av} . The inset shows a small part of the experimental island distribution and its VC's.

the surface unit cell, satisfies $A_{av} = 1/N_{av} = L_{av}^2$, and $\bar{A}_s = A_s - s$ gives the mean “free” or uncovered cell area, so $\bar{A}_{av} = (1 - \theta)A_{av}$. \bar{A}_s , rather than A_s , reflects the rate of diffusion-mediated capture, to the extent that VC’s correspond to capture areas. Figure 2(b) shows that the s dependence of \bar{A}_s/\bar{A}_{av} , for the observed range of s , is very similar to that of σ_s/σ_{av} . In fact, one finds $\sigma_s/\sigma_{av} = \alpha(\bar{A}_s/\bar{A}_{av}) + \beta$, with $\alpha \approx 1.2$ and $\beta \approx -0.2$. However, we show next that VC’s do not exactly reflect diffusion-mediated capture (which is not surprising as VC’s are a purely geometric construct).

A tessellation for which cell areas are in *exact* proportion to the capture numbers is obtained by analysis of the steady-state equation $D\nabla^2 N_1 + F = 0$, for deposition, diffusion (with coefficient $D \propto h$), and capture of adatoms, of density N_1 , by an array of islands distributed as in the experiment, in the absence of additional island nucleation [12]. At island edges we set $N_1 = 0$, corresponding to irreversible adatom capture. Given this solution, it is natural to partition the surface into “diffusion cells” (DC’s) surrounding each island, such that the lines of flux for diffusing adatoms from points within the cell flow to the appropriate island; see Fig. 3(a) which also compares DC’s with the slightly different VC’s. Across the boundaries of the DC’s the *net* surface flux of diffusing adatoms is zero. Then, it follows from Gauss’ theorem that the areas of the DC’s are in exact proportion to the capture numbers, i.e., F times a DC area gives the instantaneous growth rate of the associated island. It is also possible to further decompose the DC’s into subcells which are in exact proportion to capture numbers for individual edges of an island, as illustrated in Fig. 3(a). Flux lines in a subcell flow to the appropriate edge.

Since adatom diffusion is stochastic in nature, atoms deposited within a DC are not definitely captured by the associated island. The probability of capture decreases smoothly with distance from the island edge. This is illustrated with simulation results in Fig. 3(b). Here, dots are assigned to an island (or color) if atoms that landed on those sites, during a certain time interval, were captured by that island. Note the “fuzziness” of these sets of dots, especially near the boundaries of the DC’s. For a precise characterization, one can introduce the probability P that a diffusing adatom is captured by an island, for various starting locations on the surface. Such P ’s play the role of characteristic functions for these “fuzzy” capture zones. In the continuum limit, P satisfies the equation $\nabla^2 P = 0$, with $P = 1$ at the perimeter of the island of interest, and $P = 0$ at the perimeter of all other islands [13]. One can also introduce probabilities P_{edge} for capture at a specific island edge (where $\nabla^2 P_{edge} = 0$, and $P_{edge} = 1$ just on that edge). Figures 3(c) and 3(d) compare contours of P for two islands with the corresponding fuzzy simulation sets. Figures 3(e) and 3(f) show behavior for capture at two specific edges of one island, confirming the strong influence of the local surroundings on capture at specific edges. These results are in excellent agreement with

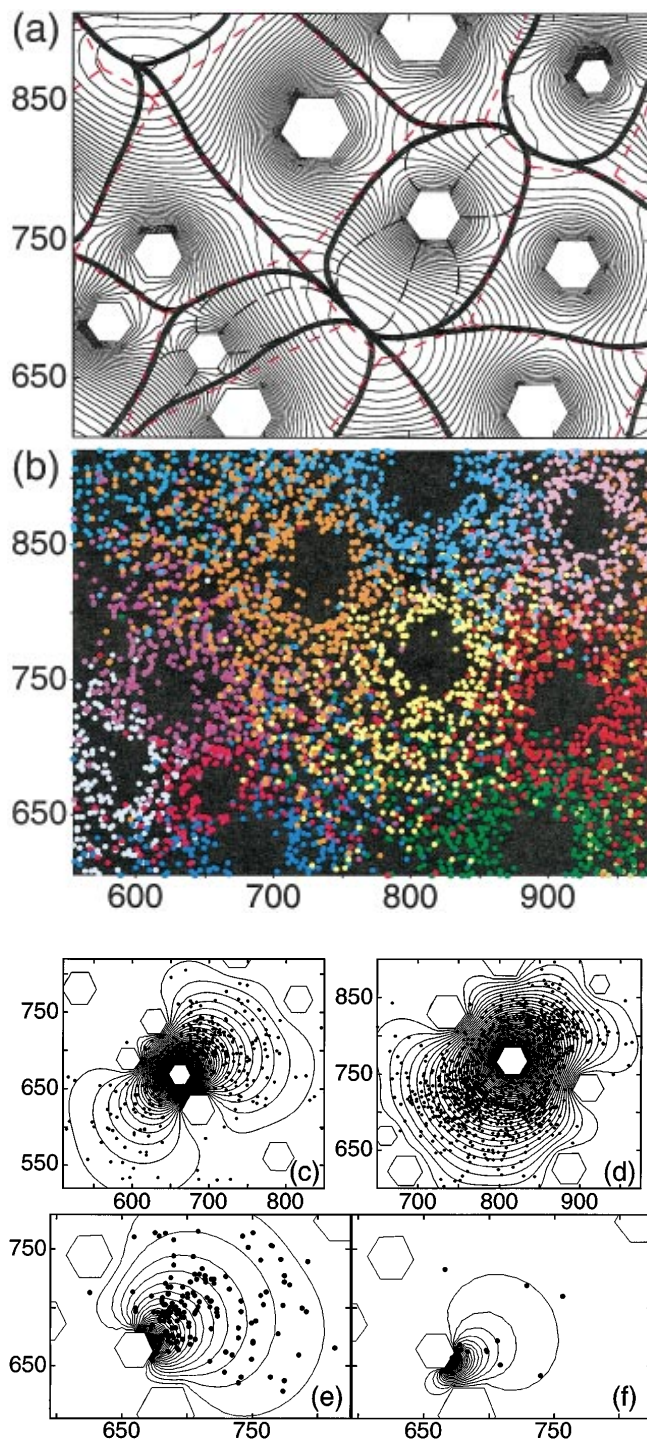


FIG. 3. Results for an island distribution matching experiment. Axes labels are in nm. (a) (color) Contours of N_1 (thin solid lines) and DC’s (bounded by thick solid lines). Edge capture cells (bounded by dashed black lines) are shown for the islands with CM at (660,669) and (816,768). VC’s (bounded by dashed red lines) are also shown. (b) (color) Simulation results: Dots, colored by island, are the landing sites of captured adatoms. (c),(d) Contours of P for the islands with CM at (660,669) in (c) and (816,768) in (d). Overlaid dots are from (b). (e),(f) Contours of P_{edge} contrasting capture for two adjacent edges of the island in (c). Dots are the landing sites of adatoms captured by each edge.

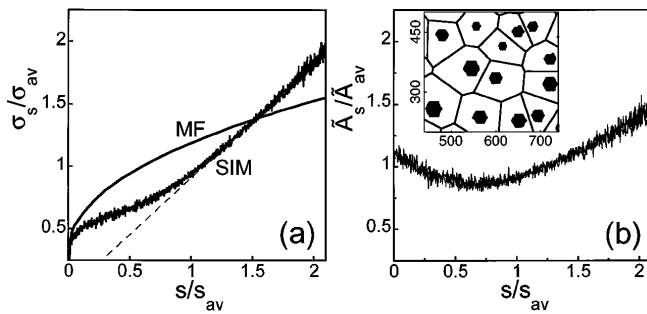


FIG. 4. Simulation (SIM) results for irreversible formation of hexagonal islands ($\theta = 0.2$ ML; $h/F = 10^8, 10^9$). (a) σ_s/σ_{av} versus s/s_{av} . The self-consistent MF form [9] is qualitatively distinct. (b) \bar{A}_s/\bar{A}_{av} versus s/s_{av} . The inset shows a small part of an island distribution for $h/F = 10^{10}$ and its VC's.

the anisotropic structure of the Cu rings observed in the experiment; cf. Fig. 1(b).

Finally, it is instructive to compare experimental behavior with results for adatom capture in a realistic “canonical” or “benchmark” model for irreversible nucleation and growth of hexagonal islands. Here, single atoms are deposited randomly on an initially empty substrate, hop to adjacent sites, and either meet other diffusing adatoms, irreversibly nucleating new (immobile) islands, or aggregate irreversibly with existing islands. After an initial “transient regime,” one finds that $N_{av} = (h/F)^{-1/3} g(\theta)$, where $g(\theta)$ depends only weakly on θ due to limited nucleation after short times, and that $N_1 \sim F/(h\sigma_{av}N_{av})$ assumes a quasisteady state. The capture rate, $h\sigma_s N_1 N_s$, for islands of size s and density N_s , is calculated from simulations as described in Ref. [5]. The results in Fig. 4 show that the form of $\sigma_s/\sigma_{av} = C(s/s_{av})$ and \bar{A}_s/\bar{A}_{av} , with s/s_{av} , is invariant with h/F , or s_{av} , at fixed θ . The simulations also show that these forms vary only weakly with θ . The form of $C()$ reproduces the simulated island size distribution choosing $\bar{\omega} \approx 0.85$ (see Ref. [5]). This size distribution is indistinguishable from that obtained for square islands [14]. The quasilinear relation between σ_s/σ_{av} and \bar{A}_s/\bar{A}_{av} for $s > s_{av}$, with $\alpha \approx 1.75$ and $\beta \approx -0.65$ reminiscent of the experiment, and the form of $C()$ is also similar to the experimental data, although the plateau in the simulated σ_s might be weaker (thus α larger). This could be due to some reversibility in Co-island nucleation in the experiment [7], and consequent differences in island spatial correlations [14], or to postdeposition coarsening in the experiment. However, we emphasize that the shape of the simulated and experimental island size distributions are consistent (within the large experimental uncertainty), and that the small number of islands in the experiment precludes meaningful analysis of experimental data for $s \lesssim s_{av}/2$.

In summary, we have characterized in detail the island size and environment dependence of Cu adatom capture by stable Co islands on Ru(0001). Combining simulations and diffusion-equation analyses, we were able to elucidate

in precise *geometric* terms details of the magnitude and direction dependence of adatom capture.

We thank N.C. Bartelt for suggesting the diffusion equation analysis for P 's. This work was supported by NSF Grant No. CHE-9700592 (J. W. E.), and by the Office of Basic Energy Science, Division of Materials Science, of the U.S. DOE Contract No. DE-AC04-94AL85000 (A. K. S., M. C. B., R. Q. H.).

- [1] M. Smoluchowski, Phys. Z. **17**, 557; **17**, 585 (1916).
- [2] *Kinetics of Aggregation and Gelation*, edited by F. Family and D. P. Landau (North-Holland, Amsterdam, 1984).
- [3] R. Q. Hwang and M. C. Bartelt, Chem. Rev. **97**, 1063 (1997).
- [4] J. A. Venables and D. J. Ball, Proc. R. Soc. London A **322**, 331 (1971); J. A. Venables, Philos. Mag. **27**, 697 (1973).
- [5] M. C. Bartelt and J. W. Evans, Phys. Rev. B **54**, R17359 (1996). If $N_s \approx \theta s_{av}^{-2} f(s/s_{av})$ denotes the density of islands of size s , and if $\sigma_s/\sigma_{av} = C(s/s_{av})$, then, for large s_{av} , one has $f(x) = f(0) \exp\{\int_0^x dy [2\bar{\omega} - 1] - C'(y)/[C(y) - \bar{\omega}y]\}$, where $\bar{\omega} = d(\ln s_{av})/d(\ln \theta)$. For irreversible island formation $\bar{\omega} \approx 2/3$ for point islands, where $N_{av} \sim \theta/s_{av} \sim \theta^{1-\bar{\omega}} \sim \theta^{1/3}$. For hexagonal islands, the enhanced tendency for saturation of N_{av} increases the effective value of $\bar{\omega}$ towards unity (hence our choice of 0.85). Also, $\bar{\omega}$ increases with the onset of reversibility in island formation.
- [6] C. Günther *et al.*, Ber. Bunsenges. Phys. Chem. **97**, 522 (1993).
- [7] At RT, we find $N_{av} \sim 840 \mu\text{m}^{-2}$, with similar flux. Assuming irreversible island nucleation, comparison with simulations [5] yields $h \sim 10^9/s$ for the effective hop rate of Co adatoms on Ru(0001) at RT. At 50 °C, simulations then obtain $N_{av} \sim 620/\mu\text{m}^{-2}$, not the observed $\sim 130 \mu\text{m}^{-2}$, so presumably island nucleation is not irreversible, or islands are mobile, at 50 °C. However, we expect Cu adatom capture by (large and far-separated) Co islands to be effectively irreversible at RT.
- [8] A. K. Schmid *et al.*, Phys. Rev. Lett. **77**, 2977 (1996).
- [9] G. S. Bales and D. C. Chrzan [Phys. Rev. B **50**, 6057 (1994)] obtain the MF form, $\sigma_s/\sigma_{av} \sim (s/s_{av})^{1/2}$, for circular islands of large size s , in contrast to the quasilinear dependence observed in experiment and simulations.
- [10] A VC is constructed by drawing the perpendicular bisecting lines to the lines joining the CM of the island to the CM's of its nearest-neighbor islands. The convex polygonal region defined by the intersection of these lines is the VC. See, e.g., F. P. Preparata and M. I. Shamos, *Computational Geometry: An Introduction* (Springer-Verlag, New York, 1985).
- [11] S. Stoyanov, Curr. Top. Mater. Sci. **3**, 421 (1979); P. A. Mulheran and J. A. Blackman, Phys. Rev. B **53**, 10261 (1996).
- [12] One could solve the discrete lattice diffusion equation, but for large island sizes and separations, as applies here, discrete lattice effects are negligible, so a continuum analysis is essentially exact.
- [13] J. W. Evans, Phys. Rev. A **40**, 2868 (1989).
- [14] M. C. Bartelt and J. W. Evans, Surf. Sci. **298**, 421 (1993); J. Vac. Sci. Technol. A **12**, 1800 (1994).